Author Manuscript

Author Manuscript

Author Manuscript

Author Manuscript

HHS Public Access

Author manuscript

Virology. Author manuscript; available in PMC 2017 January 15.

Published in final edited form as:

Virology. 2016 January 15; 488: 179–186. doi:10.1016/j.virol.2015.11.014.

The pseudorabies virus protein, pUL56, enhances virus dissemination and virulence but is dispensable for axonal transport

Gina R. Daniel[a], **Patricia J. Sollars**[b], **Gary E. Pickard**[b], and **Gregory A. Smith**[a,*]

[a]Department of Microbiology-Immunology, Northwestern University, Chicago, IL, USA

[b]School of Veterinary Medicine and Biomedical Sciences, University of Nebraska-Lincoln, Lincoln, NE, USA

Abstract

Neurotropic herpesviruses exit the peripheral nervous system and return to exposed body surfaces following reactivation from latency. The pUS9 protein is a critical viral effector of the anterograde axonal transport that underlies this process. We recently reported that while pUS9 increases the frequency of sorting of newly assembled pseudorabies virus particles to axons from the neural soma during egress, subsequent axonal transport of individual virus particles occurs with wild-type kinetics in the absence of the protein. Here, we examine the role of a related pseudorabies virus protein, pUL56, during neuronal infection. The findings indicate that pUL56 is a virulence factor that supports virus dissemination *in vivo*, yet along with pUS9, is dispensable for axonal transport.

Keywords

Herpesvirus; PRV; UL56; US9; virulence; nervous system

Introduction

The herpesviridae are a diverse family of viruses that share a core set of conserved properties [1, 2]. Their common morphology consists of a double-stranded linear DNA genome housed in an T=16 icosahedral capsid, surrounded by a proteinaceous tegument layer and membrane envelope [3]. Infections by these viruses alternate between productive and latent states, although tissue tropism and the site of latency vary across herpesviridae subfamilies and genera. For members of the simplexvirus and varicellovirus genera of the alphaherpesvirinae subfamily, latency occurs in ganglia of the peripheral nervous system (PNS). Periodic reactivation from the latent state results in nascent particle assembly and

*Corresponding author: Gregory A. Smith, Ph.D., Department of Microbiology-Immunology, Morton Bldg., Rm 3-603, Northwestern University Feinberg School of Medicine, Chicago, IL 60611, Phone: (312) 503-3745, Fax: (312) 503-5101, g-smith3@northwestern.edu.

Publisher's Disclaimer: This is a PDF file of an unedited manuscript that has been accepted for publication. As a service to our customers we are providing this early version of the manuscript. The manuscript will undergo copyediting, typesetting, and review of the resulting proof before it is published in its final citable form. Please note that during the production process errors may be discovered which could affect the content, and all legal disclaimers that apply to the journal pertain.

Author Manuscript Author Manuscript Author Manuscript Author Manuscript

subsequent transmission back to body surfaces, where virus shedding can be accompanied by mucosal or skin lesions. In rare events, infections can result in life-threatening encephalitic disease.

The transmission of viral particles outward from sensory ganglia following a reactivation event is termed anterograde axonal transport, which occurs following the induction of viral gene expression and virion assembly. Newly assembled virus particles are sorted within the cytoplasm of the neuron from the soma to the axon, and are then transported along microtubules to the distal axon terminals where the virus subsequently spreads to the innervated tissue [4, 5]. Studies of pseudorabies virus (PRV; a highly neurovirulent varicellovirus that infects a broad range of veterinary hosts, and serves as a model for encephalitic disease) and herpes simplex virus type 1 (HSV-1; a rarely neurovirulent simplexvirus that causes herpes labialis in humans) indicate that fully assembled virus particles are transported anterogradely in host vesicles [6–21]. A viral type-II transmembrane protein that is resident in the transport vesicle membrane, pUS9, serves as an effector of anterograde axonal transport for PRV and HSV-1 by augmenting the cytoplasmic sorting of viral particles into axons from the neuronal cell body [8, 22–26]. Following sorting, pUS9 remains associated with viral particles [27], but is nevertheless dispensable for the subsequent microtubule-based anterograde transport that occurs within axons [28].

The magnitude of the anterograde-deficit displayed by recombinant viruses lacking pUS9 depends on the infection model. PRV does not reach visual centers of the brain by anterograde transport from the rat retina in the absence of pUS9 [28, 29], whereas HSV-1 lacking pUS9 spreads in the same circuit within a mouse host, but at reduced levels [30]. Yet the PRV deficit is also not absolute, as PRV lacking pUS9 spreads anterogradely between nuclei within the brain [29, 31]. These findings suggest that additional viral proteins promote transport independently of pUS9. In this report, we examine the contribution of pUL56, which like pUS9 is a type-II transmembrane protein that is proposed as a candidate transport effector [32–34]. PRV strains lacking pUS9, pUL56, or both proteins were examined in cultures of primary sensory neurons and in animals. Our findings indicate that in PRV, pUL56 contributes to spread and virulence in animals, but unlike pUS9, does not contribute to axonal sorting. Furthermore, pUL56 and pUS9 provide no measurable contribution to the process of microtubule-based anterograde transport within axons.

Materials and Methods

Plasmid Construction

Recombinant PRV strains used in this study were constructed with two-step RED-mediated recombination using a pBecker3 infectious clone, GS4284, previously made to express a pUL25/mCherry capsid fusion [35–37]. To delete the UL56/ORF1.2 locus, the following primer pair was made with 5′ homologies flanking the ORF1.2 coding sequence to be deleted and 3′ homologies (underlined) to pEPkan-S2 [38]: 5′ CGCAGGTCCTGCGGGCGTACCAGATCGGTTGATGTGCGAACGATGTGACCAATA AACTCGAGGATGACGACGATAAGTAGGG and 5′ GAGACGCGGATATCGATAGGACTGGCGAGCCGAGTTTATTGGTCACATCGTTCG

Author Manuscript Author Manuscript Author Manuscript Author Manuscript

CACATCCAACCAATTAACCAATTCTGATTAG. The PCR product was recombined into infectious clone GS4284 and GS5469, the latter of which is a derivative of GS4284 deleted for the US9 gene [28]. Two-step recombination resulted in infectious clones GS4673 and GS5658 (Table 1). The deletion of ORF1.2 removed all codons following the start ATG, and preserved the stop codon and 3′ untranslated region. This deletion also removed the smaller UL56 coding sequence, which is embedded in and co-terminal with ORF1.2. The deletion was separated from the polyadenylation sequence of the downstream UL54 antisense transcript by 145 nt. Mutant viruses were initially identified by restriction enzyme analysis and confirmed by sequencing.

Cells and Viruses

PK15 cells were maintained in 10% bovine growth supplement (BGS; HyClone). During infection, the BGS concentration was reduced to 2%. Infectious clones were transfected into PK15 cells as previously described to produce stocks of recombinant PRV [39]. Working stocks were made by an additional passage through PK15 cells. Virus stocks were titered on PK15 cells as previously described [40]. Titer measurements were compiled from ≥ 3 individual working stocks. The diameters of greater than 40 plaques on PK15 cells were measured for each virus based on red capsid fluorescence emissions, and this was then repeated a total of three times for each virus. Final measurements were normalized as a percent of the parental virus plaque diameter. Single-step growth kinetics were determined as previously described [41].

Neuronal Culture

Sensory neurons were isolated from the dorsal root ganglion (DRG) of embryonic (E8–E10) chicks and cultured as previously described as either whole explants or disassociated cells [5, 42]. DRG neurons were cultured onto 22 mm^2 No. 1.5 glass coverslips treated with poly-DL-ornithine (PO). Laminin was added as a second substrate for whole explant cultures. Neuron cultures were maintained for 2–3 days with partial media change on day 2, and then infected with recombinant PRV isolates. Infections were conducted in a 2 ml volume in a well of a 6-well tissue culture tray (one coverslip per well). Explants were infected with 7–8×10^7 PFU/ml and imaged during the first hour post-infection. This provided large numbers of retrograde transport events for analysis. In contrast, dissociated neurons were infected with 2–3×10^6 PFU/ml and imaged for egress (anterograde transport) events from 10–13 hpi as previously described [7]. While this protocol limited the number of egress events that were captured, the low density of plated neurons allowed for unambiguous assessment of transport direction (anterograde vs retrograde), which is necessary during late time points when egress from primary infected neurons can be confounded by retrograde transport events following entry into a second round of cells.

Fluorescence Microscopy and Image Analysis

Virus particles were tracked in axons as described previously [43]. For virus transport experiments in dissociated or explant DRGs, imaging was done on a Nikon Eclipse TE2000-U wide-field fluorescence microscope with a 100×1.49 numerical aperture (NA) objective and a Cascade II:512 camera. Emissions from mCherry were acquired using 100-ms streaming exposures. The velocities and run lengths of virus particles moving greater than

Author Manuscript Author Manuscript Author Manuscript Author Manuscript

0.5 μm were measured with the Kymograph function in the MetaMorph software package. The ΔUL56 transport data sets presented here were conducted concurrently with a parental and ΔUS9 transport analysis that was previously published and included here for direct comparison [28]. Measurement of particle flux was performed by counting the number of capsids that passed through a defined position along the axon that was demarcated by a 5 μm perpendicular reference line, during a 30 s period.

Viral particle accumulation in axons were imaged by virtue of the mCherry-capsid reporter fusion using 1 s exposures on an inverted wide-field Nikon Eclipse TE2000-E fluorescence microscope fitted with a 60×1.4 NA objective and a Photometrics CoolSnap HQ2 camera. Experiments were repeated in triplicate. Viral particle accumulation along the length of axons was enumerated in axons whose lengths were greater than 100 μm and were as long as 450 μm; axons shorter than one field of view (100 μm) were excluded from the count. All counts were determined manually. In regions with dense capsid accumulation, counts were likely underestimates since images were taken in a single focal plane and capsids coincident with each other were only scored as a single particle. At least 6 neurons per sample were counted for the 3 hpi time point, and ≥ 20 neurons per sample were counted in total for the 15–18 hpi time point across 2 experiments. Fluorescent plaque diameters were measured with a 10x objective and 100 ms exposures.

Animal Studies

The use of animals in this study was approved by the University of Nebraska-Lincoln Institutional Animal Care and Use Committee. CD-1 mouse infection: Male mice (received from Charles River at 6 weeks of age) were acclimated to a 12:12 light:dark cycle for at least 2 weeks prior to infection. When 8–15 weeks old, animals were infected intranasally with $8–9\times10^5$ PFU/nostril (in a 5 μl volume/nostril) of PRV under 2.5% isofluorane inhalation anesthesia, as previously described [36]. Five animals were monitored per virus to determine mean time of death (MTD). A one-way ANOVA with Tukey post-test were used to determine significance. Long-Evans rat infection: Male rats (received from Charles River at 8 weeks of age) were acclimated to a 12:12 light:dark cycle for at least 2 weeks prior to infection. When 10–16 weeks old, animals were infected with PRV under 2.5% isofluorane inhalation anesthesia by unilaterally injecting either 10 μl of a $\approx 1\times10^8$ PFU/ml stock into the vitreous humor of the eye or 2 μl of the same stock into the anterior chamber of the eye, as previously described [44]. Animals were sacrificed at the indicated times by transcardial perfusion with 0.9% saline followed by 4% paraformaldehyde in 0.1 M phosphate buffer (PB). The brain and the superior cervical ganglion (SCG) ipsilateral to the injected eye were removed, post-fixed overnight at 4 C in 4% paraformaldehyde in PB with 20% sucrose. Tissue was sectioned at 30 μm on a Leica cryostat, mounted on slides, coverslipped with Vectashield and examined using a Leica DM5500 B fluorescence microscope fitted with a Hamamatsu CCD ORCA-flash 4.0 digital camera.

Author Manuscript Author Manuscript Author Manuscript Author Manuscript

Results

Initial characterization of mutant viruses

To assess the contribution of pUL56 toward neuronal infection, PRV deleted for the UL56 gene was derived from a pBecker3 infectious clone encoding a pUL25/mCherry fluorescent capsid tag. The capsid tag allows for imaging of individual viral particles in living cells [35, 36, 38]. The deletion removed the entire UL56 coding sequence and further encompassed an extended sequence referred to as ORF 1.2: a putative coding region that is in-frame and co-terminal with UL56 [45]. The resulting deletion virus, PRV-GS4673, is referred to as the ΔUL56 virus in this report (Table 1). The ΔUS9 mutant, PRV-GS5469, has the second codon through the last in-frame ATG replaced with a stop codon, and was previously described [28]. The ΔUL56 and ΔUS9 viruses remained fully competent to spread in PK15 epithelial cells (Fig. 1A) and propagated to titers equivalent to the parental strain (Fig. 1B) with normal kinetics (Fig. 1C). Consistent with prior reports, these findings document that neither pUS9 nor pUL56 significantly contribute to productive infection in non-neuronal cell culture [29, 46], and further indicate the UL56 deletion did not result in polar effects on the downstream antisense transcripts for UL52 (helicase/primase), UL53 (gK) and UL54 (ICP27), which share a poly-adenylation signal that is 145 nt downstream of the UL56 deletion [47].

Retrograde axonal transport in culture

Membrane proteins are not expected to contribute to the initial seeding of neurons by retrograde axonal transport, as this process occurs after the virion envelope is removed following fusion-based entry into axons [48]. Nevertheless, retrograde axonal trafficking was monitored to confirm that deletion of UL56 did not impair this early stage of neuronal infection [42]. Dorsal root ganglia (DRG) explants of sensory neurons were infected with either the parental fluorescent PRV strain or its ΔUL56 derivative (these experiments were conducted concurrently with the previously described ΔUS9 mutant [28]). The motion of incoming fluorescent capsids was tracked during the first hour post-infection to determine velocities and run lengths of individual viral particles, and the frequency of transport events (flux). Based on this analysis, deletion of UL56 did not perturb retrograde transport of viral particles (Fig. 2, upper panels).

Anterograde axonal transport in culture

Following replication, newly-assembled PRV particles traffic from the soma of the neuron to the axon. To obtain an accounting of viral particle sorting into axons, disassociated DRG sensory neurons were plated sparsely to limit axon interactions, and infected two days post-culturing. The number of virus particles along the length of the axon in an infected neuron, including the terminal, was enumerated at both 3 hpi (prior to the onset of anterograde axonal transport) and from 15–18 hpi [5, 7]. Unlike the sorting defect exhibited by the ΔUS9 mutant, the ΔUL56 virus produced particles that sorted into axons as efficiently as the parental strain (Fig. 3A). Furthermore, the ΔUL56 particles accumulated at the terminals of the axons by 15–18 hpi, providing an initial indication that microtubule transport within axons occurred normally (Fig. 3B–C).

Author Manuscript Author Manuscript Author Manuscript Author Manuscript

To examine the intra-axonal transport phenotype of the ΔUL56 virus more closely, individual virus particles moving in axons were recorded by time-lapse imaging and the kinetics of transport were measured. The ΔUL56 mutants transported in the anterograde direction in axons like the parental strain in terms of velocity, run length, and flux (Fig. 2, lower panels). A similar result was observed in experiments conducted in parallel with the ΔUS9 mutant [28]. Because pUS9 and pUL56 are both type-II structural membrane proteins [22, 32], a ΔUL56/ΔUS9 double-mutant virus encoding the pUL25/mCherry capsid tag (PRV-GS5658) was made to determine if the proteins possessed redundant function (Table 1). The ΔUL56/ΔUS9 virus produced plaque sizes and titers on PK15 epithelial cells equivalent to the individual mutants and the parental strain (Figure 1A, B). Like the ΔUS9 and ΔUL56 viruses, the ΔUL56/ΔUS9 recombinant remained competent for anterograde axonal transport, indicating that the engagement of kinesin motors that move PRV anterograde in axons occurs by a mechanism that is independent of these type-II membrane proteins (supplemental movie).

Virulence and dissemination in the nervous system

CD-1 mice were infected intranasally with the parental or mutant PRV strains encoding the pUL25/mCherry fusion, and the mean survival times were determined [49]. Infection with the parental PRV resulted in a mean survival time of 56.4 hours, consistent with a prior study [36]. Infection with the ΔUL56, ΔUS9, or ΔUL56/ΔUS9 virus extended mean survival times significantly, indicating that both pUL56 and pUS9 are required for full virulence in this model (Fig. 4).

To determine the degree to which the parental and mutant viruses could infect circuits via anterograde axonal transport, Long-Evans rats were infected in the vitreous humor of the eye to initiate an infection in the retinal ganglion neurons that project axons to the visual centers of the brain. This is the model traditionally used to discern transneuronal anterograde transmission defects of PRV in the mammalian nervous system, a model for which PRV requires pUS9 [25, 28, 29, 50–53]. At 48 hpi, the animals were sacrificed, and tissue sections from the eye or the retinorecipient visual centers of the brain were prepared. Infected cells were identified based on the presence of intranuclear fluorescence from newly assembled capsids containing the pUL25/mCherry tag. The transmission of the ΔUL56 virus to visual centers was equivalent to the parental strain, indicating that pUL56 is not required for transneuronal spread following anterograde axonal transport in the mammalian nervous system (Fig. 5). This result extends the anterograde trafficking results obtained in cultured sensory neurons (Figs. 2 & 3), but does not account for the virulence defect of the ΔUL56 mutant observed in mice (Fig. 4). Therefore, we next examined the neuroinvasive property of the ΔUL56 mutant in a retrograde circuit.

Long-Evans rats were infected by injecting either the parental, ΔUL56, ΔUS9, or the ΔUL56/ΔUS9 virus into the anterior chamber of the eye. In this model, viral replication initially occurs in the iris and ciliary body, which precedes entry into axons innervating these tissues and retrograde axonal transport to peripheral ganglia, including the superior cervical ganglion (SCG) [43]. The rat SCG contains ≈ 30,000 neurons, of which 600–1000 project directly to the eye [54]. At the indicated times, animals were sacrificed,

Author Manuscript Author Manuscript Author Manuscript Author Manuscript

transcardially perfused, and the SCG ipsilateral to the injected eye was removed and prepared for microscopic examination. Infection with the parental virus resulted in labeling of > 5000 neurons in the SCG, indicating infection had surpassed the initial seeding of the ganglion. In contrast, although the ΔUS9 and ΔUL56/ΔUS9 viruses seeded the SCG, the number of infected neurons did not surpass the number of neurons that project to the eye, consistent with these infections being restricted to neurons that innervated the eye directly. This may be explained by the reduced capacity of the ΔUS9 viruses to engage in anterograde axonal transport, which should effectively imprison the virus in the initially seeded SCG neurons. Although the ΔUL56 mutant did not share the ΔUS9 sorting defect, it presented an intermediate defect in the number of neurons infected in the SCG, indicating that pUL56 enhances infection of the peripheral nervous system (Fig. 6).

Discussion

To transmit between hosts, a latent neuroinvasive herpesvirus infection must reactivate and send newly-assembled viral particles from peripheral sensory ganglia to body surfaces by anterograde axonal transport. The same process can, in rare instances, result in transmission of infection from sensory neurons to the central nervous system (CNS), resulting in life-threatening encephalitic disease [55]. Because reactivation from latency is normally sporadic and of varying magnitude, anterograde axonal transport is typically studied in models of acute infection. Thus, in a CNS invasive model of infection based on inoculating PRV in the vitreous chamber of the rat eye, virus infects local neurons in the retina (retinal ganglion cells) and then transmits within these neurons to the brain by anterograde axonal transport. For PRV, the pUS9 type-II membrane protein is often referred to as an essential determinant for anterograde axonal transmission because ΔUS9 mutants of PRV fail to spread to the brain in this rat eye model [29]. However, pUS9 is not essential in all contexts. For example, in an intracranial model of CNS infection, pUS9 is dispensable for anterograde axonal transport between distal nuclei within the brain [29].

Anterograde axonal transport consists of two steps. First, nascent cytoplasmic viral particles are sorted from the cell body into the axon. Once in the axon, the particles transport to the terminal by plus-end directed microtubule transport. The latter is sustained over distances of several centimeters to nearly a meter [56]. In the absence of pUS9, the initial step of PRV sorting into axons occurs infrequently [27]; however, the few PRV particles that transport in the absence of pUS9 do so with kinetics that are indistinguishable from PRV encoding pUS9 [28]. Because ΔUS9 PRV can sustain long-distance transport within axons to spread anterogradely in the intracranial model and in cultured primary neurons, this indicates that additional effectors of axonal transport may exist [8, 28, 29].

A second type-II transmembrane protein, pUL56, was suggested to have transport effector functions based on studies of HSV-2 [32, 33, 57]. Although pUL56 was described initially in HSV, phylogenetic studies have identified a UL56 ortholog in PRV, previously called ORF-1 [58]. We chose to delete ORF-1/UL56 along with the an overlapping and co-terminal coding sequence called ORF1.2, to effectively rule out either as encoding effectors of axonal transport. Deletion of UL56 and ORF1.2 from PRV did not impair viral replication in epithelial cells, in agreement with previous reports [46]. The retrograde axonal transport

Author Manuscript Author Manuscript Author Manuscript Author Manuscript

kinetics of the mutant were equivalent to the parental strain following entry into primary cultured neurons and the kinetics were also unperturbed for anterograde transport during neuronal egress, with the latter culminating in normal accumulation of PRV particles at axon terminals. These findings were consistent with the subsequent studies in animals, where the mutant was not impaired for infection of visual centers of the rat brain via anterograde transport from the eye. We conclude that pUL56 (and products from ORF1.2) is not an effector of PRV anterograde transport in primary cultured neurons or *in vivo*. Unlike pUS9, pUL56 did not promote initial sorting of cytoplasmic PRV particles into axons, and neither pUS9 nor pUL56 (deleted individually or together) were required for intra-axonal transport of particles beyond the sorting barrier.

Whether other viral effectors of kinesin-based anterograde trafficking encoded by PRV contribute to post-sorting anterograde axonal transport remains an open question. Because PRV transports anterogradely as a fully-assembled virus particle within the lumen of a transport vesicle, there may be no need for a virally-encoded transport effector during this stage of infection if the vesicle is targeted to the axon terminal by the cell. However, there are reports that in addition to vesicle-based anterograde transport, HSV-1 may uniquely be able to transport as a proteinaceous capsid/tegument particle directly in the cytosol of the axon [4, 21]. In this scenario, HSV-1 would require a direct effector of kinesin recruitment. In either scenario, the pUL36 large tegument protein is an interesting candidate effector based on its role in kinesin-based transport of capsids *in vitro* [59].

Whereas deletion of UL56 had no impact on anterograde transport *in vivo*, infection of peripheral ganglia, a retrograde circuit, was attenuated. This reduction in infection was not accounted for in the culture studies where defects in propagation, spread, and axonal transport were not observed. Nevertheless, the defect corresponded to reduced virulence; in fact, in the mouse intranasal model, ΔUL56 infection was more attenuated than infection by the ΔUS9 virus. pUL56 has multiple reported functions in related alphaherpesviruses, including modulation of cell-surface markers, regulation of cellular ubiquitin ligases, and interaction with viral proteins that ultimately interact with glycoprotein E [57, 60–68]. These interactions could promote innate immune evasion in the host. Further studies will be needed to identify the mechanism by which pUL56, and possibly products of ORF1.2, contributes to virulence.

Supplementary Material

Refer to Web version on PubMed Central for supplementary material.

Acknowledgments

This work was supported by NIH grant R01 AI056346 to G.A.S. and R01 NS077003 to G.E.P. and P.J.S. G.R.D was supported by the training program in the Cellular and Molecular Basis of Disease from the National Institutes of Health (T32 GM08061). We thank Anne Fischer and Stephanie Totten for excellent technical assistance, and Jenifer Klabis for help with figure illustrations.

Author Manuscript Author Manuscript Author Manuscript Author Manuscript

References

1. Davison AJ, Eberle R, Ehlers B, Hayward GS, McGeoch DJ, Minson AC, Pellett PE, Roizman B, Studdert MJ, Thiry E. The order Herpesvirales. Arch Virol. 2009; 154(1):171–7. [PubMed: 19066710]
2. McGeoch DJ, Rixon FJ, Davison AJ. Topics in herpesvirus genomics and evolution. Virus Res. 2006; 117(1):90–104. [PubMed: 16490275]
3. Pellet, PE.; Roizman, B.; Knipe, DM.; Whitley, RJ. Fields' Virology. 5. Knipe, DMHPM., editor. Lippincott-Williams and Wilkins; New York: 2007.
4. Miranda-Saksena M, Armati P, Boadle RA, Holland DJ, Cunningham AL. Anterograde transport of herpes simplex virus type 1 in cultured, dissociated human and rat dorsal root ganglion neurons. J Virol. 2000; 74(4):1827–39. [PubMed: 10644356]
5. Smith GA, Gross SP, Enquist LW. Herpesviruses use bidirectional fast-axonal transport to spread in sensory neurons. Proc Natl Acad Sci U S A. 2001; 98(6):3466–70. [PubMed: 11248101]
6. Antinone SE, Smith GA. Two modes of herpesvirus trafficking in neurons: membrane acquisition directs motion. J Virol. 2006; 80(22):11235–40. [PubMed: 16971439]
7. Antinone SE, Zaichick SV, Smith GA. Resolving the assembly state of herpes simplex virus during axon transport by live-cell imaging. J Virol. 2010; 84(24):13019–30. [PubMed: 20810730]
8. Ch'ng TH, Enquist LW. Neuron-to-cell spread of pseudorabies virus in a compartmented neuronal culture system. J Virol. 2005; 79(17):10875–89. [PubMed: 16103140]
9. Cook ML, Stevens JG. Pathogenesis of herpetic neuritis and ganglionitis in mice: evidence for intra-axonal transport of infection. Infect Immun. 1973; 7(2):272–88. [PubMed: 4348966]
10. Feierbach B, Bisher M, Goodhouse J, Enquist LW. In vitro analysis of transneuronal spread of an alphaherpesvirus infection in peripheral nervous system neurons. J Virol. 2007; 81(13):6846–57. [PubMed: 17459934]
11. del Rio T, Ch'ng TH, Flood EA, Gross SP, Enquist LW. Heterogeneity of a fluorescent tegument component in single pseudorabies virus virions and enveloped axonal assemblies. J Virol. 2005; 79(7):3903–19. [PubMed: 15767393]
12. Field HJ, Hill TJ. The pathogenesis of pseudorabies in mice following peripheral inoculation. J Gen Virol. 1974; 23(2):145–57. [PubMed: 4833604]
13. Hill TJ, Field HJ, Roome AP. Intra-axonal location of herpes simplex virus particles. J Gen Virol. 1972; 15(3):233–5. [PubMed: 4114320]
14. Kristensson K, Ghetti B, Wisniewski HM. Study on the propagation of Herpes simplex virus (type 2) into the brain after intraocular injection. Brain Res. 1974; 69(2):189–201. [PubMed: 4362812]
15. LaVail JH, Topp KS, Giblin PA, Garner JA. Factors that contribute to the transneuronal spread of herpes simplex virus. J Neurosci Res. 1997; 49(4):485–96. [PubMed: 9285524]
16. Lycke E, Hamark B, Johansson M, Krotochwil A, Lycke J, Svennerholm B. Herpes simplex virus infection of the human sensory neuron. An electron microscopy study. Arch Virol. 1988; 101(1–2):87–104. [PubMed: 2843151]
17. Lyman MG, Feierbach B, Curanovic D, Bisher M, Enquist LW. Pseudorabies virus Us9 directs axonal sorting of viral capsids. J Virol. 2007; 81(20):11363–71. [PubMed: 17686845]
18. Maresch C, Granzow H, Negatsch A, Klupp BG, Fuchs W, Teifke JP, Mettenleiter TC. Ultrastructural analysis of virion formation and anterograde intraaxonal transport of the alphaherpesvirus pseudorabies virus in primary neurons. J Virol. 2010; 84(11):5528–39. [PubMed: 20237081]
19. Negatsch A, Granzow H, Maresch C, Klupp BG, Fuchs W, Teifke JP, Mettenleiter TC. Ultrastructural analysis of virion formation and intraaxonal transport of herpes simplex virus type 1 in primary rat neurons. J Virol. 2010; 84(24):13031–5. [PubMed: 20943987]
20. Huang J, Lazear HM, Friedman HM. Completely assembled virus particles detected by transmission electron microscopy in proximal and mid-axons of neurons infected with herpes simplex virus type 1, herpes simplex virus type 2 and pseudorabies virus. Virology. 2011; 409(1):12–6. [PubMed: 21036381]

Author Manuscript Author Manuscript Author Manuscript Author Manuscript

21. Wisner TW, Sugimoto K, Howard PW, Kawaguchi Y, Johnson DC. Anterograde transport of herpes simplex virus capsids in neurons by both separate and married mechanisms. J Virol. 2011; 85(12):5919–28. [PubMed: 21450818]
22. Brideau AD, Banfield BW, Enquist LW. The Us9 gene product of pseudorabies virus, an alphaherpesvirus, is a phosphorylated, tail-anchored type II membrane protein. J Virol. 1998; 72(6):4560–70. [PubMed: 9573219]
23. Snyder A, Polcicova K, Johnson DC. Herpes simplex virus gE/gI and US9 proteins promote transport of both capsids and virion glycoproteins in neuronal axons. J Virol. 2008; 82(21):10613–24. [PubMed: 18753205]
24. Howard PW, Howard TL, Johnson DC. Herpes simplex virus membrane proteins gE/gI and US9 act cooperatively to promote transport of capsids and glycoproteins from neuron cell bodies into initial axon segments. J Virol. 2013; 87(1):403–14. [PubMed: 23077321]
25. LaVail JH, Tauscher AN, Sucher A, Harrabi O, Brandimarti R. Viral regulation of the long distance axonal transport of herpes simplex virus nucleocapsid. Neuroscience. 2007; 146(3):974–85. [PubMed: 17382478]
26. Kratchmarov R, Enquist LW, Taylor MP. Axonal sorting and transport of the pseudorabies virus glycoprotein gM independent of Us9. J Virol. 2015
27. Taylor MP, Kramer T, Lyman MG, Kratchmarov R, Enquist LW. Visualization of an alphaherpesvirus membrane protein that is essential for anterograde axonal spread of infection in neurons. MBio. 2012; 3(2)
28. Daniel GR, Sollars PJ, Pickard GE, Smith GA. Pseudorabies Virus Fast Axonal Transport Occurs by a pUS9-Independent Mechanism. J Virol. 2015; 89(15):8088–91. [PubMed: 25995254]
29. Brideau AD, Card JP, Enquist LW. Role of pseudorabies virus Us9, a type II membrane protein, in infection of tissue culture cells and the rat nervous system. J Virol. 2000; 74(2):834–45. [PubMed: 10623746]
30. McGraw HM, Awasthi S, Wojcechowskyj JA, Friedman HM. Anterograde spread of herpes simplex virus type 1 requires glycoprotein E and glycoprotein I but not Us9. J Virol. 2009; 83(17): 8315–26. [PubMed: 19570876]
31. Card JP, Levitt P, Enquist LW. Different patterns of neuronal infection after intracerebral injection of two strains of pseudorabies virus. J Virol. 1998; 72(5):4434–41. [PubMed: 9557737]
32. Koshizuka T, Goshima F, Takakuwa H, Nozawa N, Daikoku T, Koiwai O, Nishiyama Y. Identification and characterization of the UL56 gene product of herpes simplex virus type 2. J Virol. 2002; 76(13):6718–28. [PubMed: 12050385]
33. Koshizuka T, Kawaguchi Y, Nishiyama Y. Herpes simplex virus type 2 membrane protein UL56 associates with the kinesin motor protein KIF1A. J Gen Virol. 2005; 86(Pt 3):527–33. [PubMed: 15722511]
34. Rosen-Wolff A, Lamade W, Berkowitz C, Becker Y, Darai G. Elimination of UL56 gene by insertion of LacZ cassette between nucleotide position 116030 to 121753 of the herpes simplex virus type 1 genome abrogates intraperitoneal pathogenicity in tree shrews and mice. Virus Res. 1991; 20(3):205–21. [PubMed: 1662844]
35. Smith GA, Enquist LW. A self-recombining bacterial artificial chromosome and its application for analysis of herpesvirus pathogenesis. Proc Natl Acad Sci U S A. 2000; 97(9):4873–8. [PubMed: 10781094]
36. Bohannon KP, Sollars PJ, Pickard GE, Smith GA. Fusion of a fluorescent protein to the pUL25 minor capsid protein of pseudorabies virus allows live-cell capsid imaging with negligible impact on infection. J Gen Virol. 2012; 93(Pt 1):124–9. [PubMed: 21976610]
37. Tischer BK, Smith GA, Osterrieder N. En Passant Mutagenesis: A Two Step Markerless Red Recombination System. 2010; 634:421–430.
38. Tischer BK, von Einem J, Kaufer B, Osterrieder N. Two-step red-mediated recombination for versatile high-efficiency markerless DNA manipulation in Escherichia coli. Biotechniques. 2006; 40(2):191–7. [PubMed: 16526409]
39. Luxton GW, Haverlock S, Coller KE, Antinone SE, Pincetic A, Smith GA. Targeting of herpesvirus capsid transport in axons is coupled to association with specific sets of tegument proteins. Proc Natl Acad Sci U S A. 2005; 102(16):5832–7. [PubMed: 15795370]

Author Manuscript Author Manuscript Author Manuscript Author Manuscript

40. Smith GA, Enquist LW. Construction and transposon mutagenesis in Escherichia coli of a full-length infectious clone of pseudorabies virus, an alphaherpesvirus. J Virol. 1999; 73(8):6405–14. [PubMed: 10400733]
41. Tirabassi RS, Enquist LW. Role of envelope protein gE endocytosis in the pseudorabies virus life cycle. J Virol. 1998; 72(6):4571–9. [PubMed: 9573220]
42. Smith GA, Pomeranz L, Gross SP, Enquist LW. Local modulation of plus-end transport targets herpesvirus entry and egress in sensory axons. Proc Natl Acad Sci U S A. 2004; 101(45):16034–9. [PubMed: 15505210]
43. Zaichick SV, Bohannon KP, Hughes A, Sollars PJ, Pickard GE, Smith GA. The herpesvirus VP1/2 protein is an effector of dynein-mediated capsid transport and neuroinvasion. Cell Host Microbe. 2013; 13(2):193–203. [PubMed: 23414759]
44. Lee JI, Sollars PJ, Baver SB, Pickard GE, Leelawong M, Smith GA. A herpesvirus encoded deubiquitinase is a novel neuroinvasive determinant. PLoS Pathog. 2009; 5(4):e1000387. [PubMed: 19381253]
45. Klupp BG, Hengartner CJ, Mettenleiter TC, Enquist LW. Complete, annotated sequence of the pseudorabies virus genome. J Virol. 2004; 78(1):424–40. [PubMed: 14671123]
46. Baumeister J, Klupp BG, Mettenleiter TC. Pseudorabies virus and equine herpesvirus 1 share a nonessential gene which is absent in other herpesviruses and located adjacent to a highly conserved gene cluster. J Virol. 1995; 69(9):5560–7. [PubMed: 7637001]
47. Schwartz JA, Brittle EE, Reynolds AE, Enquist LW, Silverstein SJ. UL54-null pseudorabies virus is attenuated in mice but productively infects cells in culture. J Virol. 2006; 80(2):769–84. [PubMed: 16378979]
48. Nicola AV, Hou J, Major EO, Straus SE. Herpes simplex virus type 1 enters human epidermal keratinocytes, but not neurons, via a pH-dependent endocytic pathway. J Virol. 2005; 79(12): 7609–16. [PubMed: 15919913]
49. Klopfleisch R, Teifke JP, Fuchs W, Kopp M, Klupp BG, Mettenleiter TC. Influence of tegument proteins of pseudorabies virus on neuroinvasion and transneuronal spread in the nervous system of adult mice after intranasal inoculation. J Virol. 2004; 78(6):2956–66. [PubMed: 14990714]
50. Pickard GE, Smeraski CA, Tomlinson CC, Banfield BW, Kaufman J, Wilcox CL, Enquist LW, Sollars PJ. Intravitreal injection of the attenuated pseudorabies virus PRV Bartha results in infection of the hamster suprachiasmatic nucleus only by retrograde transsynaptic transport via autonomic circuits. J Neurosci. 2002; 22(7):2701–10. [PubMed: 11923435]
51. Dingwell KS, Doering LC, Johnson DC. Glycoproteins E and I facilitate neuron-to-neuron spread of herpes simplex virus. J Virol. 1995; 69(11):7087–98. [PubMed: 7474128]
52. Husak PJ, Kuo T, Enquist LW. Pseudorabies virus membrane proteins gI and gE facilitate anterograde spread of infection in projection-specific neurons in the rat. J Virol. 2000; 74(23): 10975–83. [PubMed: 11069992]
53. Card JP, Whealy ME, Robbins AK, Moore RY, Enquist LW. Two alpha-herpesvirus strains are transported differentially in the rodent visual system. Neuron. 1991; 6(6):957–69. [PubMed: 1711350]
54. Strack AM, Loewy AD. Pseudorabies virus: a highly specific transneuronal cell body marker in the sympathetic nervous system. J Neurosci. 1990; 10(7):2139–47. [PubMed: 1695943]
55. Smith G. Herpesvirus transport to the nervous system and back again. Annu Rev Microbiol. 2012; 66:153–76. [PubMed: 22726218]
56. Tannous R, Grose C. Calculation of the anterograde velocity of varicella-zoster virions in a human sciatic nerve during shingles. J Infect Dis. 2011; 203(3):324–6. [PubMed: 21186259]
57. Koshizuka T, Kawaguchi Y, Goshima F, Mori I, Nishiyama Y. Association of two membrane proteins encoded by herpes simplex virus type 2, UL11 and UL56. Virus Genes. 2006; 32(2):153–63. [PubMed: 16604447]
58. Davison AJ. Herpesvirus systematics. Vet Microbiol. 2010; 143(1):52–69. [PubMed: 20346601]
59. Shanda SK, Wilson DW. UL36p is required for efficient transport of membrane-associated herpes simplex virus type 1 along microtubules. J Virol. 2008; 82(15):7388–94. [PubMed: 18495763]

Author Manuscript Author Manuscript Author Manuscript Author Manuscript

60. Ushijima Y, Luo C, Kamakura M, Goshima F, Kimura H, Nishiyama Y. Herpes simplex virus UL56 interacts with and regulates the Nedd4-family ubiquitin ligase Itch. Virol J. 2010; 7:179. [PubMed: 20682038]

61. Ushijima Y, Goshima F, Kimura H, Nishiyama Y. Herpes simplex virus type 2 tegument protein UL56 relocalizes ubiquitin ligase Nedd4 and has a role in transport and/or release of virions. Virol J. 2009; 6:168. [PubMed: 19835589]

62. Ushijima Y, Koshizuka T, Goshima F, Kimura H, Nishiyama Y. Herpes simplex virus type 2 UL56 interacts with the ubiquitin ligase Nedd4 and increases its ubiquitination. J Virol. 2008; 82(11): 5220–33. [PubMed: 18353951]

63. Said A, Azab W, Damiani A, Osterrieder N. Equine herpesvirus type 4 UL56 and UL49.5 proteins downregulate cell surface major histocompatibility complex class I expression independently of each other. J Virol. 2012; 86(15):8059–71. [PubMed: 22623773]

64. Han J, Chadha P, Meckes DG Jr, Baird NL, Wills JW. Interaction and interdependent packaging of tegument protein UL11 and glycoprotein e of herpes simplex virus. J Virol. 2011; 85(18):9437–46. [PubMed: 21734040]

65. Huang T, Lehmann MJ, Said A, Ma G, Osterrieder N. Major histocompatibility complex class I downregulation induced by equine herpesvirus type 1 pUL56 is through dynamin-dependent endocytosis. J Virol. 2014; 88(21):12802–15. [PubMed: 25165105]

66. Huang T, Ma G, Osterrieder N. Equine Herpesvirus 1 Multiply Inserted Transmembrane Protein pUL43 Cooperates with pUL56 in Downregulation of Cell Surface Major Histocompatibility Complex Class I. J Virol. 2015; 89(12):6251–63. [PubMed: 25833055]

67. Claessen C, Favoreel H, Ma G, Osterrieder N, De Schauwer C, Piepers S, Van de Walle GR. Equid herpesvirus 1 (EHV1) infection of equine mesenchymal stem cells induces a pUL56-dependent downregulation of select cell surface markers. Vet Microbiol. 2015; 176(1–2):32–9. [PubMed: 25582614]

68. Soboll Hussey G, Ashton LV, Quintana AM, Van de Walle GR, Osterrieder N, Lunn DP. Equine herpesvirus type 1 pUL56 modulates innate responses of airway epithelial cells. Virology. 2014; 464–465:76–86.

Author Manuscript Author Manuscript Author Manuscript Author Manuscript

- pUL56 and pUS9 type-II membrane proteins are encoded by neuroinvasive herpesviruses
- pUL56 and pUS9 are virulence factors that enhance seeding of the nervous system
- Unlike pUS9, pUL56 does not contribute to sorting of virus into axons
- Intra-axonal transport of PRV particles occurs independently of both proteins

Author Manuscript Author Manuscript Author Manuscript Author Manuscript

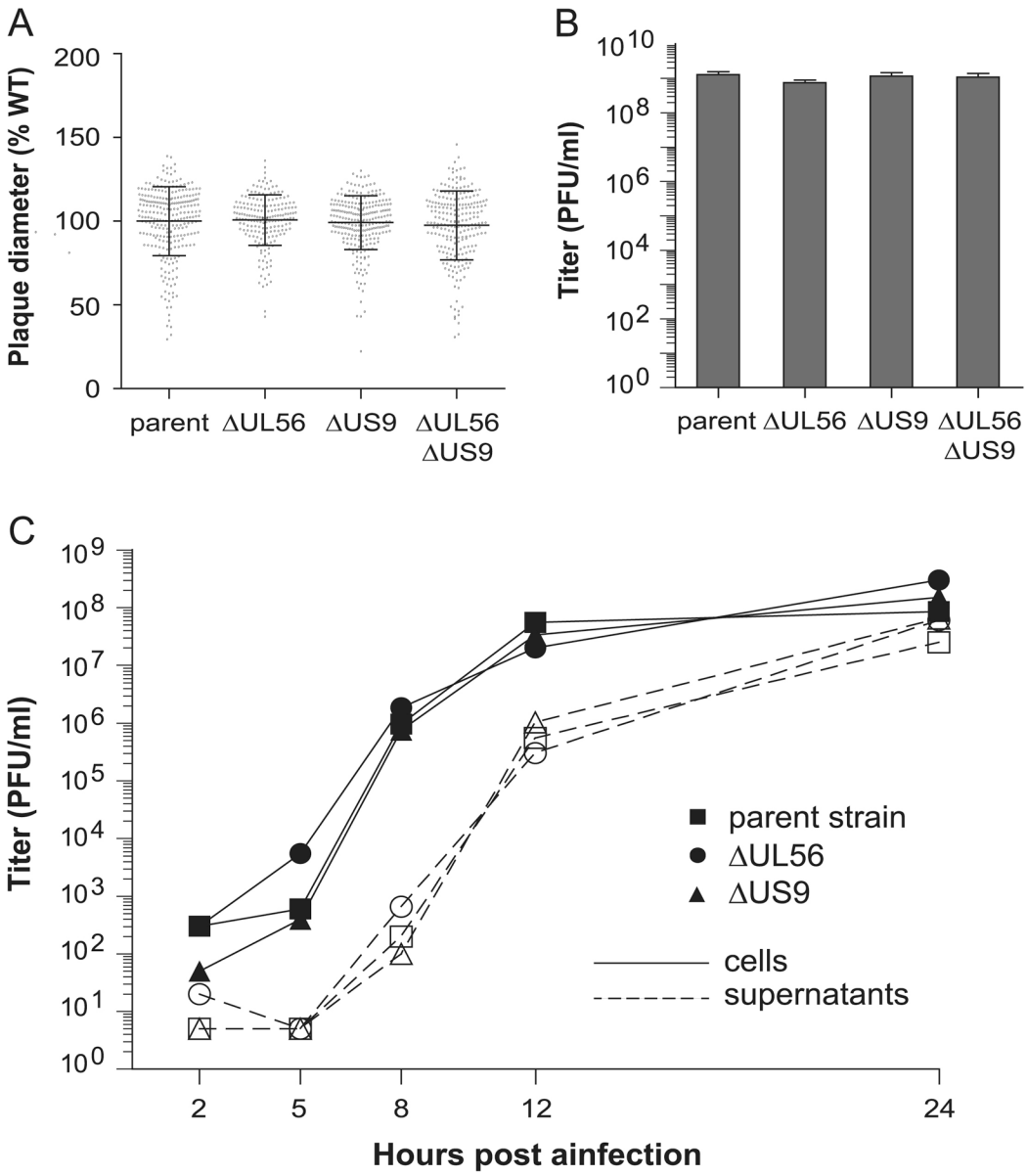

Figure 1. Deletion of UL56 or US9 from PRV does not impair replication in the PK15 epithelial cell line

Plaque diameters (A) and titers (B) were measured on PK15 cells after infection with the parent PRV strain or derivatives lacking UL56 or US9, singly or in combination. (A) Greater than 40 plaques were measured per experiment and experiments were repeated in triplicate (error bars indicate standard deviation). (B) Titer measurements were compiled from three or more viral stocks (error bars indicate standard error of the mean). (C) Single-step replication kinetics of parental, ΔUL56, or ΔUS9 infection was determined by collecting infected cells or infected cell supernatants at the indicated times, followed by plaque assay to determine titer.

Author Manuscript Author Manuscript Author Manuscript Author Manuscript

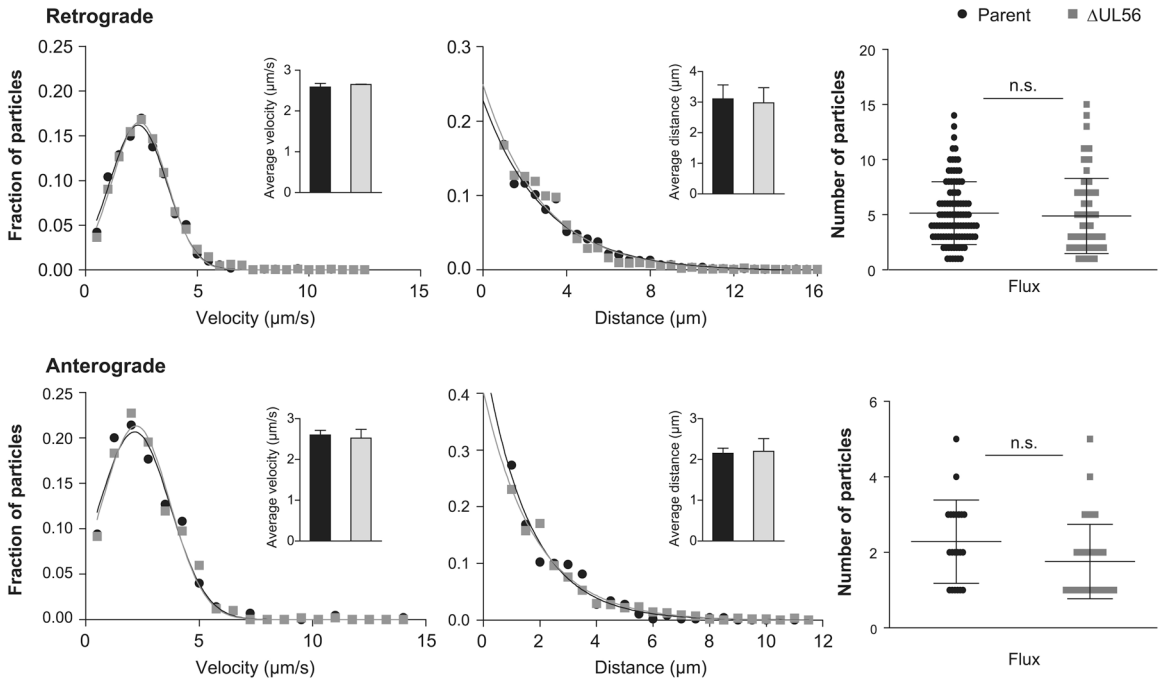

Figure 2. Deletion of UL56 from PRV does not alter retrograde or anterograde transport dynamics of viral particles in culture

Primary sensory neurons were infected with the parental strain or ΔUL56 PRV and pUL25/mCherry capsids were imaged during ingress from 15–60 min post infection (upper panels) and during egress from 10–13 hpi (lower panels). Viral particles moving in axons greater than 0.5 μm were tracked and individual velocities and run lengths were measured during ingress (parent, n=288; ΔUL56, n=175) and egress (parent, n=38; ΔUL56, n=48). Gaussian (velocities) or decaying exponential (run lengths) curves were fit to histograms by non-linear regression; for all experiments, curve-fitting produced R^2 values > 0.96. Insets show average velocity (left panels) and run length (middle panels); error bars indicate standard error of the mean. The frequency of capsid axonal transport events (flux) was measured as the number of capsids moving per axon over a 30 s period during ingress (parent, n=99; ΔUL56, n=70) and egress (parent, n=21; ΔUL56, n=37) (right panels); error bars indicate standard deviation.

Author Manuscript Author Manuscript Author Manuscript Author Manuscript

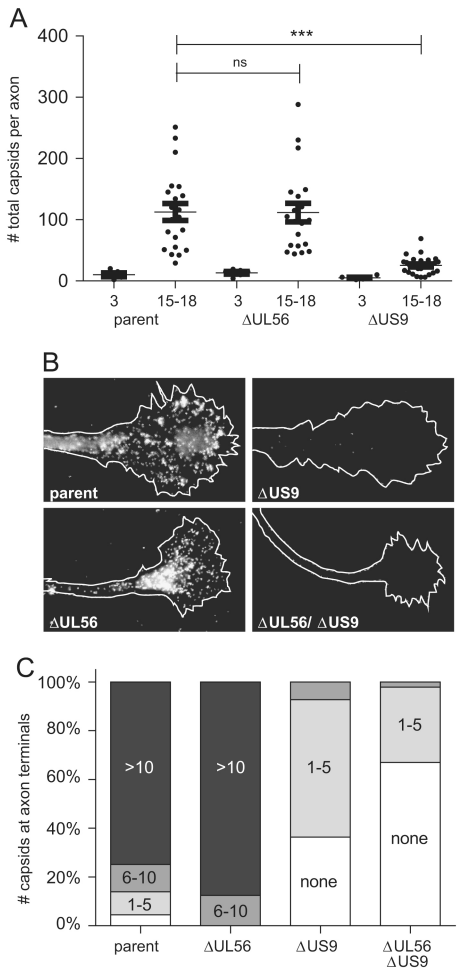

Figure 3. Deletion of US9, but not UL56, results in diminished accumulation of viral particles at axon terminals late in infection

(A) Sparsely seeded dissociated primary sensory neurons were infected with parental, ΔUL56, or ΔUS9 PRV, and the number of fluorescent capsids localized along the length of individual axons were counted at 3 hpi and 15–18 hpi. Only infected neurons extending axons > 100 μm that could be traced for their entire length were included in the analysis. Error bars indicate standard deviation. Significance was determined with one-way ANOVA and Tukey's post-test. (B) Primary sensory neurons were infected with parental, ΔUL56, ΔUS9, or ΔUL56/ΔUS9 virus and the distal ends of the neurons were imaged between 15–18 hpi. (C) The abundance of viral particles at axon terminals is reported as a frequency based on the number of capsids observed per terminal (parent, n=213; ΔUL56, n=45; ΔUS9, n=109; ΔUL56/ΔUS9, n=236).

Author Manuscript Author Manuscript Author Manuscript Author Manuscript

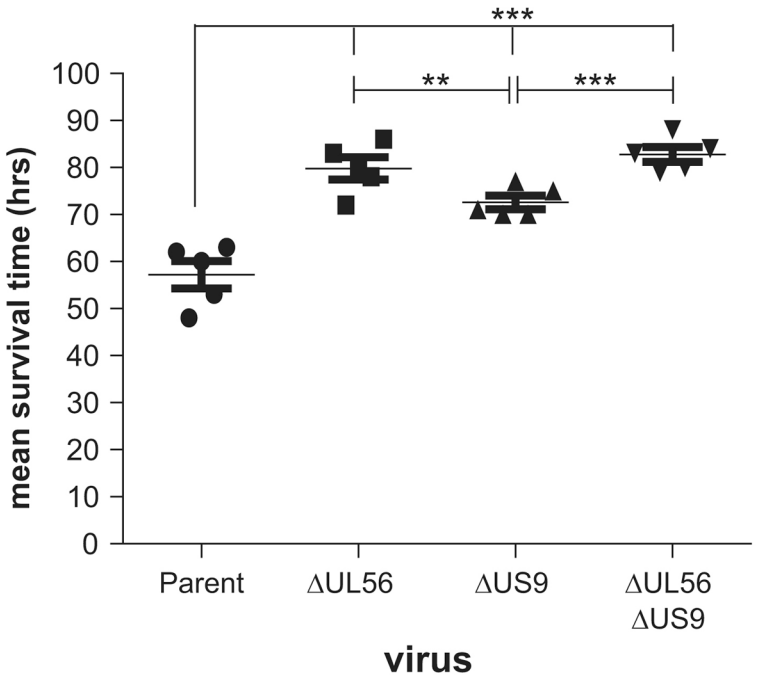

Figure 4. Contributions of pUS9 and pUL56 to PRV virulence

Five CD-1 mice were infected by intranasal instillation with each virus, and mean survival times were determined. A one-way ANOVA with Tukey post-test was used to determine significance.

Author Manuscript Author Manuscript Author Manuscript Author Manuscript

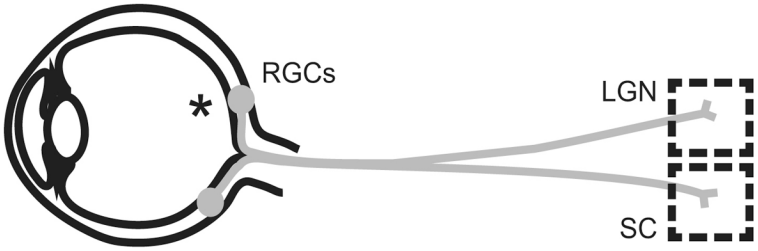

		Retina	Visual Centers of the Brain
Virus	Animal	RGC	LGN/SC
Parent	1	+	+
	2	+	+
	3	+	+
ΔUL56	1	+	+
	2	+	+
	3	+	+

Figure 5. pUL56 is dispensable for anterograde spread of PRV in rat visual circuits

Long Evans rats were infected by intravitreal injection with parental, ΔUL56, or ΔUS9 PRV. The location of the injection in the eye is indicated by an asterisk (*). At 48 hpi, the animals were sacrificed. Peripheral tissue sections of the eye, including retinal ganglion cells (RGC), or brain sections of retinorecipient visual centers, including the lateral geniculate nucleus (LGN) and superior colliculus (SC), were examined for infected neurons, indicated by red-fluorescence emissions from the pUL25/mCherry capsid fusion. For each infection, three animals were examined. A (+) indicates the presence of red-fluorescent/infected cells.

Author Manuscript Author Manuscript Author Manuscript Author Manuscript

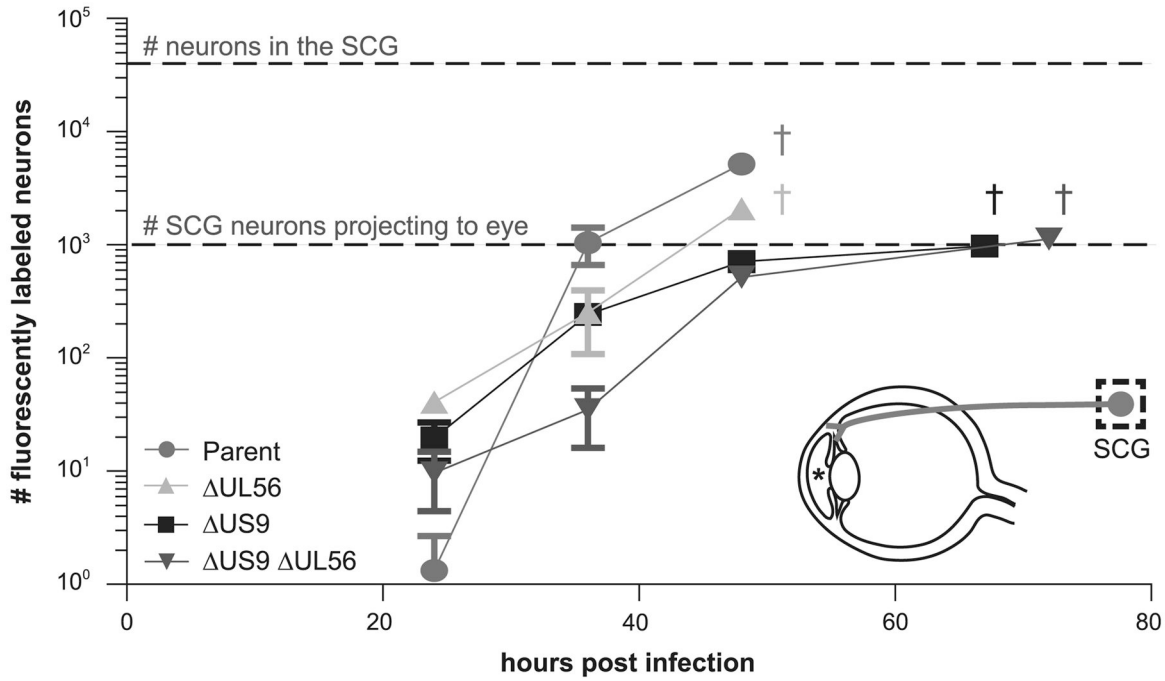

Figure 6. pUL56 promotes infection of the superior cervical ganglion

Parental, ΔUL56, ΔUS9, or a ΔUL56/ΔUS9 double-mutant virus was injected into the anterior chamber of the eye of male Long Evans rats. The location of the injection in the eye is indicated by an asterisk (*). Animals were sacrificed at the indicated times and the superior cervical ganglion (SCG) was removed, sectioned, and scored for infected neurons based on red-fluorescence emissions from the pUL25/mCherry capsid fusion. The symbol '†' denotes the time of imminent death from infection. The lower dashed line indicates the number of neurons in the SCG that project directly to the eye. The upper dashed line indicates the total number of neurons, ≈ 30,000, that comprise the SCG.

Author Manuscript
Author Manuscript
Author Manuscript
Author Manuscript

Table 1

Viruses used in this study

Virus	Reporter Tag	Mutation	Moniker	Source
PRV-GS4284	pUL25/mCherry	-	parent	Bohannon, 2012
PRV-GS4673	pUL25/mCherry	ΔUL56 ΔORF1.2	ΔUL56	this study
PRV-GS5469	pUL25/mCherry	ΔUS9	ΔUS9	Daniel, 2015
PRV-GS5658	pUL25/mCherry	ΔUL56 ΔORF1.2 ΔUS9	ΔUL56/ΔUS9	this study